GAVIN PUBLISHERS

Nanomedicine and Nanoscience Research

Research Article

Chun Shen, et al. J Nanomed Nanosci: JNAN-105.
DOI: 10.29011/JNAN-105.100005

Steam Reforming of Toluene on Ni/Phyllosilicate: Enhanced Catalytic Activity and Stability

Chun Shen*, Hao Yu, Wuqing Zhou, Shina Ma, Tianwei Tan

Beijing University of Chemical Technology, Chaoyang, Beijing, PR China

***Corresponding author:** Chun Shen, Beijing Key Laboratory of Bioprocess, College of Life Science and Technology, Beijing University of Chemical Technology, No. 15 of North Three-Ring East Road, Chaoyang District, Beijing 100029, PR China. Tel: +8618001181869; Email: shenchun@mail.buct.edu.cn

Citation: Shen C, Yu H, Zhou W, Ma S, Tan T (2017) Steam Reforming of Toluene on Ni/Phyllosilicate: Enhanced Catalytic Activity and Stability. J Nanomed Nanosci: JNAN-105. DOI: 10.29011/JNAN-105.100005

Received Date: 13 July, 2016; **Accepted Date:** 23 July, 2017; **Published Date:** 1 August, 2017

Abstract

Aimed at steam reforming of tar model compounds (toluene), we specially designed and prepared phyllosilicate supported with Ni nanoparticle acting as the heterogeneous catalyst. Because of the confinement effect of the lamellar structure of phyllosilicate and the presence of strong interaction between phyllosilicate and Ni, highly dispersed Ni nanoparticles supported on phyllosilicate were obtained showing excellent catalytic activity and anti-sintering property. The mean diameter of Ni nanoparticles varied from 3.3 to 6.0 nm with the loading amount increased from 17.4 wt.% to 31.3 wt.%. 100% conversion of toluene was obtained under the reaction conditions (reaction temperature: 923 K, catalyst weight to flow rate: 0.72 g□h□mol^{-1}, steam to carbon ratio: 3). And the conversion just decreased from 100% to 90% after 660 min. Overall, as the highly active and stable catalyst, Ni/SiO_{2P} provided an alternative for efficient steam reforming of tar.

Keywords: Catalytic Performance; Ni Nanoparticles; Steam Reforming; Strong Metal-Support Interaction

Introduction

Reported by the Energy White Paper of the Australian Department of Resource, Energy and Tourism, the world global energy demand in year 2035 will be higher than current level [1]. Nowadays, the majority of our energy derived from the consumption of fossil fuels, which will release pollutants to the atmosphere and lead to a series of environmental problems such as greenhouse effect and NOx emissions [2-4]. So, it urged to develop renewable clean energy [5].

Biomass gasification is one of the most important technologies for the conversion of biomass to electricity, fuels, and chemicals [6-9]. However, this potential technology is limited by tar formation in the total process. In general, tar is complex and high-molecular weight compounds containing more than 10,000 species of aromatic which will impair the engine by deposition in the engine [10]. The reduction of tar content is the major point to utilize gasification technology successfully. Catalytic steam reforming is considered as the most effective method for reducing tar [11-15].

Heterogeneous catalysts are widely used in steam reforming of tar because of their easy separation and recycle. Noble metals such as Pt [16], Rh [16,17], Ru [18], Pd [19] and Ir [20] manifest high activity in steam reforming. However, the noble metals are inappropriate for industrial application because of the high cost and rapid deactivation. Thus, it is of great significance to develop supported based-metal catalyst with excellent activity and stability.

Supported Ni catalysts are drawing more and more attention because of the cheap cost and high activity [21-29]. In Zhang's work [27], Ni-Ce-Mg/olivine was used as the catalyst for steam reforming of toluene. The highest conversion of 93% was reached with the reaction temperature of 1063K, catalyst weight to flow rate (W/F) of 11.4g.h.mol^{-1}, and steam to carbon ratio (S/C) of 3.5. Mukai and coworkers [28] reported that Ni/$La_{0.7}Sr_{0.3}AlO_{3-\delta}$ showed high activity for steam reforming of toluene. The conversion of 72.9% was reached under the reaction conditions (reaction temperature was 1073K, W/F was 3.4 g.h.mol^{-1}, S/C was 2). However, it is reported that Ni nanoparticles tended to sinter resulting in deactivation during the steam reforming.

In order to solve the problem, great efforts have been paid to enhance the interaction between the supported metal [30-39]. According to Li and coworkers [36], alkaline-promoted Nial-Montmorillonite (NiAl-Mt) catalysts prepared by ion-exchange

method showed high metal-support interaction and stability. However, it is difficult to obtain supported Ni nanoparticles with small mean particles size when the Ni loading amount is high through this approach. As reported by P. Burattin [37-39], the highly dispersed Ni nanoparticles supported on Phyllosilicate (PS) prepared by Deposition-Precipitation (DP) method, showed great stability. The excellent anti-sintering property of PS-derived catalysts could be ascribed to the confinement effect of the lamellar structure and the presence of Strong Metal-Support Interaction (SMSI). The Ni nanoparticles were highly dispersed with the average particle size of only 4.7 nm with the Ni content of 11.7 wt% However, nickel phyllosilicate (Ni/SiO_{2P}) is relatively less studied in catalytic reforming processes [33].

In this paper, synthesis, characterization and activity test of Ni/SiO_{2P} are reported. As far as we know, application of Ni/SiO_{2P} to steam reforming of toluene has never been reported before. There may be three possible advantages by choosing PS as the support: first, because of the SMSI, it is easier to obtain highly dispersed Ni nanoparticles with high loading amount (for example 26.8 wt.%) which would be of great help for the promotion of the catalytic activity; second, the confinement effect of the lamellar structure and the presence of SMSI would lead to the excellent anti-sintering property and stability; third, PS is low cost and environmental friendly providing promising alternative for heterogeneous Ni-based catalysts. The Ni/SiO_{2P} was prepared by the DP method using silicone gel as the silicon source, and reduced with H_2. X-Ray Diffraction (XRD), Transmission Electron Microscope (TEM), H_2-Temperature Programmed Reduction (H_2-TPR) and Brunauer-Emmett-Teller (BET) analysis were used to characterize the structure and superficial properties of the Ni/SiO_{2P}.Catalytic activity and stability are investigated for the steam reforming of toluene. Effects of residence time, S/C ratio, and Ni content have been studied systematically in relation to the change in the conversion. And the stability of the as-prepared catalyst was investigated as well.

Experimental

Materials

Ammonium Hydroxide [$NH_3 \cdot H_2O$, 25%] and SiO_2 were purchased from Sinopharm Chemical Reagent Co., LTD. Silica sol with 30 percent was purchased from Shandong peak-tech materials Co., LTD. Nickle (II) nitrate [$Ni(NO_3)_2 \cdot 6H_2O$] was purchased from Fuchen Chemical Plant in Tianjin. The commercial ZSM-5 catalyst was purchased from the Catalyst Plant of Nankai University. Toluene was purchased from Beijing Chemical Plant.

Catalyst preparation and characterization

The Ni/SiO_{2P} catalyst was prepared by DP method [33]. A certain amount of $Ni(NO_3)_2 \cdot 6H_2O$ and 8.4mL of $NH_3 \cdot H_2O$ were dissolved in 80mL of deionized water, which were placed in a tank reactor and stirred at room temperature. 6 g of silica sol was added in the Ni-contain solution and stirred for 6 h at room temperature. Hereafter, the tank reactor was gradually heated to 353 K with stirred to evaporate ammonia. Nickel species were deposited on silica with the decrease of pH, and the tank reactor was cooled to room temperature when the pH value was below 7. Afterword the suspension was filtered by vacuum filtration and washed several times by deionized water. Finally, the solid was dried at 373 K for 12 h and reduced by hydrogen at 873 K.

The Ni/SiO_2 catalyst and Ni/ZSM-5 catalyst was prepared by wetness impregnation method. A certain amount of $Ni(NO_3)_2 \cdot 6H_2O$ and SiO_2 were dissolved in 100mL of deionized water. After magnetic stirred for 2 h at room temperature, the Ni-containing solution was heated to 353 K to evaporate water. The resultant solid was dried at 373 K for 12 h, followed by reduction by hydrogen at 873 K.

The calcined powders were studied by XRD using a Bruker D8-Advance X-ray diffractometer with Cu K α radiation (λ=0.154nm). The machine operated over a range of 2θ angles from 10° to 90°. The crystalline size was evaluated by the Scherrer's equation: D=0.89λ/(β=cosθ). The specific surface area and pore structure were detected using Brunauer-Emmett-Teller (BET) analysis by nitrogen adsorption isotherms at 77K using a Micromeritics ASAP 2020 surface analyzer. H_2-TPR was performed by heating the catalysts to 1266 K with the heating rate of 5 K/min in 10% hydrogen and the total flow rate was 30 mL/min. TEM was used to characterize the size of particle.

Catalytic tests

The steam reforming of toluene was performed in a fixed bed quartz reactor with internal diameter was 6mm. 0.3g of catalyst was fixed in the middle of quartz reactor. Water and toluene were fed into the reactor by injection pumps and vaporized before contact with the catalyst. N_2 with the flow rate of 30mL/min was used as the carrier gas. The products were flow through acetone and then collected by an airbag. Gas Chromatograph (GC) with a Flame Ionization Detector (FID) was used to analyze the organic species in acetone and GC with a Thermal Conductivity Detector (TCD) was used to analyze the gas in the airbag. The toluene conversion (X) and gas production selectivity were calculated by Equation (1) and (2),

$$X(\%) = \frac{n_{in} - n_{out}}{n_{in}} \times 100 \quad (1)$$

$$S_i(\%) = \frac{n_i}{n_{H_2} + n_{CO} + n_{CO_2} + n_{CH_4}} \times 100 \quad (2)$$

Where X is the conversion of toluene, n_{in} is the mole of toluene and n_{out} is the mole of unreacted toluene S_i is the selectivity of *i*.

Results and Discussion

Characteristics of Ni-based catalysts

In order to makes comparisons, Ni nanoparticles were also supported on ZSM-5 zeolite and SiO_2 by the impregnation method. The structural properties and surface morphology of our catalysts are shown in (Table 1) and (Figure 1) respectively. The specific surface area of Ni/SiO_{2P} is 435.0 m^2/g. And the pore volume and the average pore diameter are 0.92 mL/g and 8.4nm, respectively. Compared with Ni/SiO_2 and Ni/ZSM-5, the Ni/SiO_{2P} catalyst shows larger specific surface area and pore volume. (Figure 1) shows the N_2 adsorption-desorption isotherms of the catalysts. The hysteresis loops indicated the existence of mesoporous.

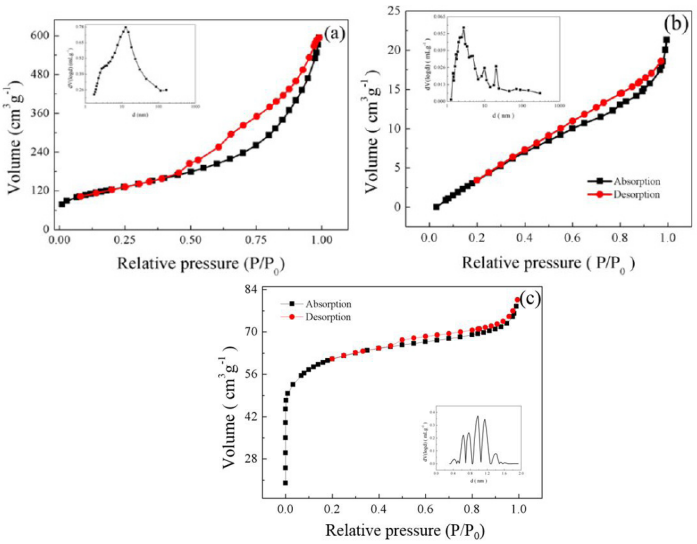

Figure 1: N_2 Adsorption-Desorption Isotherms and BJH Mesopore Size Distribution (Inset) of Catalysts with Ni Content Of 26.8 W%; (A): Ni/PS, (B): Ni/SiO_2; (C): Ni/ZSM-5.

XRD patterns of Ni/SiO_2P, Ni/SiO_2 and Ni/ZSM-5catalysts are shown as (Figure 2).

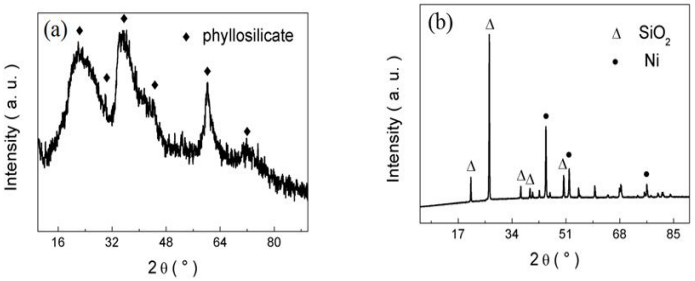

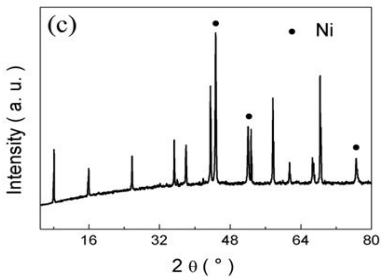

Figure 2: XRD Pattern of Catalysts with Ni Content Of 25 Wt.%; (A): Ni/PS; (B) Ni/SiO_2; (C) Ni/ZSM-5.

Diffraction peaks at 21.6˚, 30.2˚, 35.6˚, 44.0˚, 60.4˚, and 71.3˚ are contributed to the (111), (110), (220), (222), (121), (130) facets of PS support, respectively [40-41]. Due to the small size and good dispersion of Ni nanoparticles supported on SiO_2 by the DP method, the peak of Ni was difficult to discern. On the other hand, diffraction peaks at 44.5˚,51.8˚, and76.4˚ appeared in the patterns of Ni/ZSM-5 and Ni/SiO_2 are contributed to (111), (200), and (220) facets of nickel nanoparticles. Diffraction peaks at 21.0˚, 26.7˚, 36.6˚, 39.7˚ and 50.4˚ of Ni/SiO_2 are contributed to the facets of SiO_2. The crystal Ni nanoparticle size of Ni/ZSM-5 and Ni/SiO_2 shown in (Table 1) were calculated to be 27 nm and 25 nm, respectively according to the Scherrer's equation.

(Figure 3) shows the H_2-TPR results of Ni/SiO_2P, Ni/SiO_2 and Ni/ZSM-5. Ni/ZSM-5 showed two reduction peaks at around 559K and around 573 K, which are attributed to the reduction of NiO.

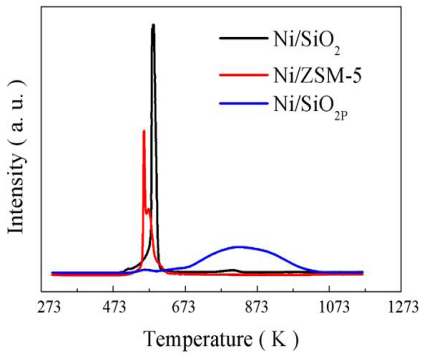

Figure 3: H2-TPR Results of the As-Prepared Catalysts.

As for Ni/SiO_2, the main reduction peak around 583K can be ascribed to the reduction of NiO particles, the peak around 798 K could be assigned to the Ni^{2+} ions interacting with SiO_2. Two reduction peaks could also be observed in the result of Ni/SiO_2P,

Catalyst	Ni content (wt.%)	SA[a] (m^2/g)	PD[b] (nm)	PV[c] (cm^2/g)	D(Ni)[d] (nm)
Ni/SiO2P	26.8	436.00	8.40	0.92	-
Ni/SiO2	26.8	409.10	3.20	0.03	25
Ni/ZSM-5	26.8	183.80	2.44	0.12	27
a: Specific surface, b: average pore diameter, c: pore volume, d: Ni nanoparticle size determined from XRD.					

the small peak at 561 K could be ascribed to the reduction of NiO particles, while Ni^{2+} located in phyllosilicates were reduced at around 823K [42]. The highest main reduction peak of Ni/SiO_{2P} indicated the strongest metal-support interaction which would be benefit for the preparation of Ni nanoparticles with small size and narrow distribution. TEM images of the as-prepared catalysts are shown in (Figure 4).

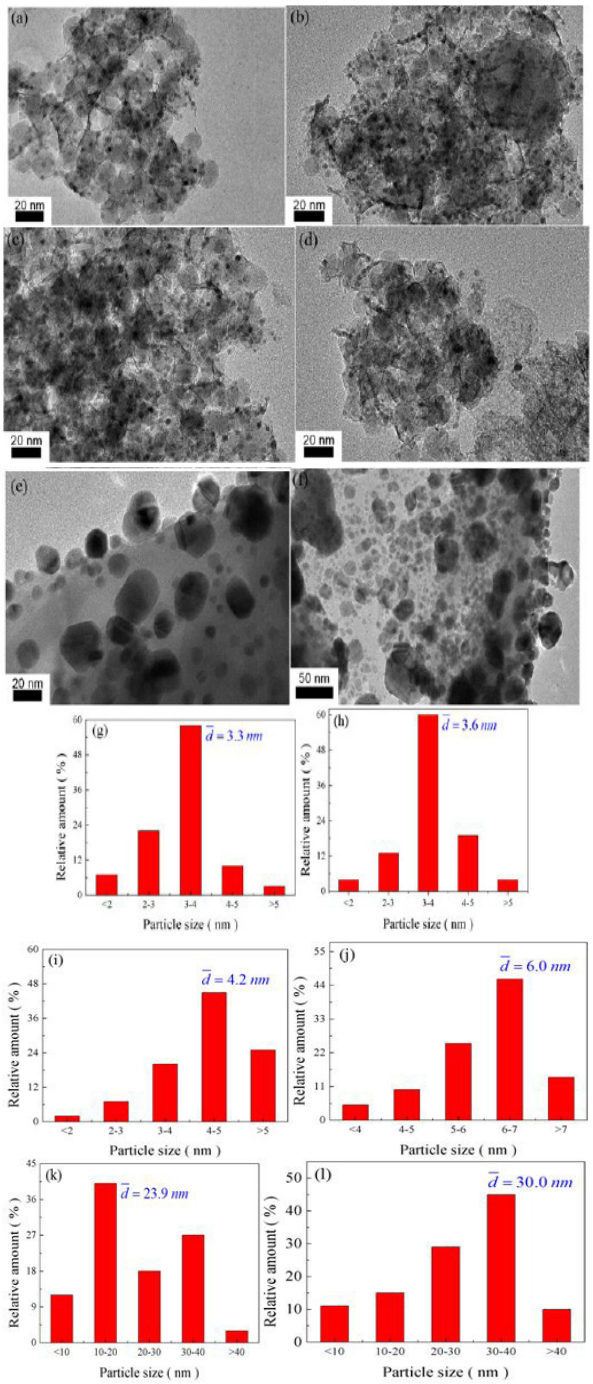

Figure 4(a-l): TEM Images of Catalysts; (a), (b), (c), and (d): Ni/SiO_{2P} with Ni Content of 17.4 wt.%, 22.4 wt.%, 26.8 wt.%, 31.3 wt.%; (e): Ni/SiO2 with Ni Content of 26.8%; (f): Ni/ZSM-5 with Ni Content of 26.8%;(g), (h), (i), (j), (k), and (l): Histograms of Particle Size Distribution for Ni/SiO_2P, Ni/ SiO_2, and Ni/ ZSM-5, respectively.

The perfectly formed structure of PS and mesoporous could be clearly observed. TEM images of Ni nanoparticles supported on PS with Ni content of 17.4 wt.%, 22.4 wt.%, 26.8 wt.%, 31.3 wt.% are shown as (Figure 4(a), 4(b), 4(c), and 4(d)), respectively. And TEM images of Ni/SiO_2 and Ni/ZSM-5 catalysts with the Ni content of 24 wt.% are shown as (Figure 4(e) and 4(f)) respectively. The corresponding distribution histograms of Ni nanoparticles are shown as (Figure 4(g), 4(h), 4(i), 4(j), 4(k), 4(l)) respectively. The histograms were derived from corresponding TEM images by more than 100 particles. The mean crystal nickel particle size is calculated using the equation ($\bar{d} = \sum n_i d_i / \sum n_i$, where n_i is the number of corresponding nickel particles with a diameter of d_i.). The mean particles size of Ni nanoparticles are3.3nm, 3.6 nm, 4.2 nm and 6.0 nm for catalysts with Ni contents of 17.4 wt.%, 22.4 wt.%, 26.8 wt.%, and 31.3 wt.%, respectively. And the mean diameters of Ni particles supported on SiO_2 and ZSM-5 are 23.9 nm and 30.0 nm, respectively. Obviously, as expected, Ni nanoparticles supported on PS exhibited small mean particle size and narrow size distribution which might be of great help for improving the catalytic activity and stability.

Effect of residence time on conversion

As shown in (Figure 5), the effect of residence time on conversion was investigated.

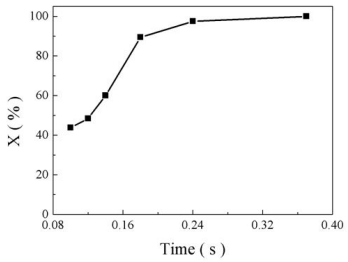

Figure 5: Effect of Residence Time on Conversion; Reaction Temperature: 923K; 0.3 G Catalyst; Ni Content: 31.6 Wt.%; Toluene Feed Rate: 2ml/H; S/C: 1; The Flow Rate of N_2: 30ml/Min.

With the increase of residence time, the conversion of toluene increased gradually. The conversion was only 43.8% when the residence time was 0.1s, and the conversion rapidly increased to 99% when the residence time increased to 0.37s. Longer residence time means longer reaction duration, so the conversion would increase as well. TEM image of the used catalyst is shown as (Figure 5) in the supporting material. After the catalytic reaction, Ni nanoparticles still highly dispersed on the surface of PS.

Effect of S/C on conversion

As shown in (Figure 6), catalytic performances under different S/C values were determined.

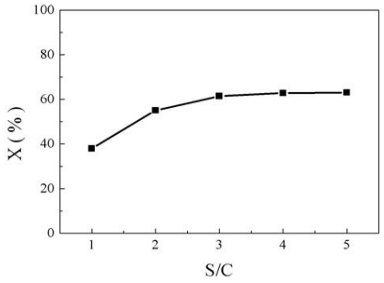

Figure 6: Effect of S/C on Conversion; Reaction Temperature: 923K; 0.3 G Catalyst; Ni Content: 31.6 Wt.%; Toluene Feed Rate: 2ml/H; the Flow Rate of N_2: 30ml/Min.

When the S/C ratio was not higher than 3, the conversion of toluene increased with the increase of S/C ratio. And the conversion remained constant when the S/C ratio further increased. This could be explained as follows, the Equation (3) and (4) were promoted by the increase of water. So, the conversion of toluene will increase with the increase of S/C. But when the S/C was beyond 3, the conversion of toluene will not be improved because under these values of S/C, the main restrictive factor for steam reforming reaction was not the amount of steam, but the active sites of catalysts. Therefore, the S/C ratio was kept as 3 for subsequent research.

$$C_7H_8 + 7H_2O \rightarrow 7CO + 11H_2 \quad (3)$$

$$CO + H_2O \rightarrow CO_2 + H_2 \quad (4)$$

Effect of Ni content on conversion

Catalytic performances of Ni/SiO_{2P} catalysts with various Ni contents are shown in (Figure 7).

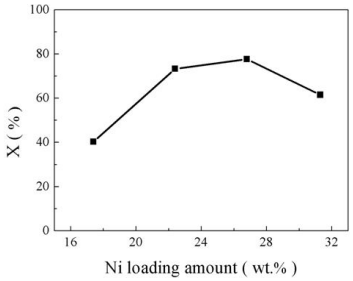

Figure 7: Effect of Ni Content on Conversion; Reaction Temperature: 923K; 0.3 G Catalyst; S/C: 3; Toluene Feed Rate: 4ml/H; The Flow Rate of N_2: 30ml/Min.

The conversion of toluene increased from 45% to 78% when the Ni content increased from 21.0 wt.% to 26.8 wt.%. However, further increase in Ni content resulted in reduction of reaction rate. Catalyst with the highest Ni content of 31.3 wt.% showed even worse performance than that of the catalyst with the Ni content of 26.8 wt.%. This may be driven by two factors: first, with the increase of the loading amount, the Ni particle size increased to almost 6.0 nm decreasing the catalytic activity (as shown in (Figure 4(d)); second, only the Ni nanoparticles loaded on the outer part played a role during the reaction.

Catalysts stability study

The catalytic stability of our catalysts was studied. The performances of Ni/SiO_{2P}, Ni/SiO_2 and Ni/ZSM-5are shown in (Figure 8, 9, and 10), respectively.

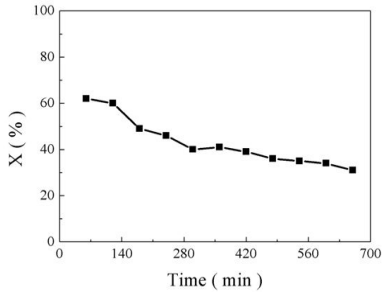

Figure 9: Catalysts Stability Study on Ni/SiO_2; Reaction Temperature: 923K; 0.3 G Catalyst; S/C: 3; Ni Content: 26.8 Wt.%; Toluene Feed Rate: 2ml/H; The Flow Rate of N_2: 30ml/Min.

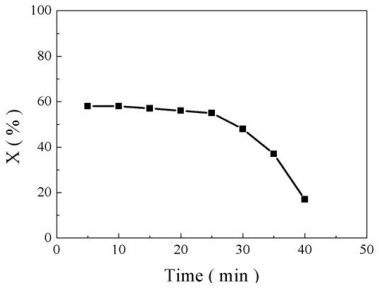

Figure 10: Catalysts Stability Study on Ni/ZSM-5; Reaction Temperature: 923K; 0.3 G Catalyst; S/C: 3; Ni Content: 26.8 Wt.%; Toluene Feed Rate: 2ml/H; The Flow Rate of N_2: 30ml/Min.

As shown in (Figure 8), the initial toluene conversion reached 100%, and kept at 90% even after 660 min. The main gas production is H2 with the selectivity of around 60%. Comparatively, Ni/SiO2 and Ni/ZSM-5 showed much worse stability for the steam reforming of toluene. For Ni/ZSM-5, the initial conversion was58%, and the conversion is rapidly decreased. And the conversion of toluene was only 62%, and the conversion decreased to 31% after 660 min using Ni/SiO_2 as the catalyst. Above all, Ni/SiO_{2P} showed the highest catalytic activity and the best stability. Steam reforming of toluene has also been investigated in other works. According to Quitetea [43], the conversion of toluene decreased from 78% to 59% after 660 min. Comparisons in catalytic performances with other works are listed in (Table 2) [27,44,45]. Therefore, the PS supported with Ni nanoparticles showed high catalytic activity and stability.

s	Reaction temperature (K)	Toluene conversion (%)	TOF×10^4 (s^{-1})	Reference
Ni/SiO_{2P}	923	99	17.0	This work
$Ni/La_{0.7}Sr_{0.3}AlO_{3-\delta}$	873	92	5.8	[43]
Ni/Ce/Mg/olivine	1005	93	4.8	[27]
Ni-Mn/dolomite	1073	65	1	[44]

Table 2: Comparisons in Catalytic Performance with Other Works.

Conclusion

PS supported with Ni nanoparticles was successfully prepared and acted as a novel heterogeneous catalyst for steam reforming of toluene. Compared with Ni/SiO_2 and Ni/ZSM-5, the Ni/SiO_{2P} catalyst prepared in this work showed smaller Ni nanoparticles size and narrower size distribution. The mean Ni nanoparticle size of Ni/SiO_{2P} varied from 3.3 to 6.0nm with the loading amount increased from 17.4 wt.% to 31.3 wt.%. The pore volume, pore size and specific surface area of Ni/SiO_{2P} were 0.92 mL/g, 8.40 nm and 436.0 m^2/g, respectively. Effects of residence time, S/C and Ni content on conversion were studied systematically. The conversion increased with the increase of residence time. The increase of S/C could also improve the conversion of toluene. The Ni content was optimized to be 26.8 wt.%. The as-prepared Ni/SiO_{2P} catalysts showed high catalytic activity and stability. The conversion of toluene reached 100% under the reaction conditions (reaction temperature was 923 K; 0.3 g catalyst; S/C was 3; Ni content of 26.8 wt.%; toluene feed rate was 2mL/h). And the conversion of toluene just decreased from 100% to 90% after 660 min.

Acknowledgements

We gratefully acknowledge the support of the National Nature Science Foundation of China (21606008, 21436002), the National Basic Research Foundation of China (973 program) (2013CB733600), the Fundamental Research Funds for the Central Universities (ZY1630, JD1617), and the Fundamental Research Funds for the Central Universities (buctrc201616, buctrc201617).

References

1. Draft Energy White Paper (2011) Strengthening mumullen the foundations for Australia's energy future. Department of Resources, Energy and Tourism.
2. Holladay J, Hu J, King D, Wang Y (2009) An overview of hydrogen production technologies. Catal Today 139: 244-260.
3. Navarro RM, Pena MA, Fierro JLG (2007) Hydrogen production reactions from carbon feedstocks: Fossils fuels and biomass. Chem Rev 107: 3952-3991.
4. Navarro RM, Sanchez-Sanchez MC, Alvarez-Galvan MC, Valle FD, Fierro JLG (2009) Hydrogen production from renewable sources: biomass and photocatalytic opportunities. Energy Environ Sci 2: 35-54.
5. Tekin K, Karagöz S, Bektaş S (2014) A review of hydrothermal biomass processing. Renew Sust Energ Rev 40: 673-687.
6. Norskov JK, Christensen CH (2008) Toward Efficient Hydrogen Production at Surfaces. Science 312: 1322-1323.
7. Li DI, Tamura M, Nakagawa Y, Tomishige K (2015) Metal catalysts for steam reforming of tar derived from the gasification of lignocellulosic biomass. Bioresour Technol 178: 53-64.
8. Ashok J, Kathiraser Y, Ang ML, Kawi S (2015) Bi-functional hydrotalcite-derived NiO-CaO-Al_2O_3 catalysts for steam reforming of biomass and/or tar model compound at low steam-to-carbon conditions. Appl Catal B 172-173: 116-128.
9. Erkiaga A, Lopez G, Amutio M, Bilbao J, Olazar M (2014) Influence of operating conditions on the steam gasification of biomass in a conical spouted bed reactor. Chem Eng J 237: 259-267.
10. Laosiripojana N, Sutthisripok W, Charojrochkul S, Assabumrungrat S (2014) Development of Ni-Fe bimetallic based catalysts for biomass tar cracking/reforming: Effects of catalyst support and co-fed reactants on tar conversion characteristics. Fuel Process Technol 127: 26-32
11. Anis S and Zainal ZA (2011) Tar reduction in biomass producer gas via mechanical, catalytic and thermal methods: a review. Renew Sust Energ Rev 15: 2355-2377.
12. Shen Y and Yoshikawa K (2013) Recent progresses in catalytic tar elimination during biomass gasificationor pyrolysis-A review. Renew Sust Energy Rev 21: 371-392.
13. Yoon SJ, Kim YK, Lee JG (2011) Catalytic oxidation of biomass tar over platinum and Ru catalysts. Ind Eng Chem Res 50: 2445-2451.
14. Bona S, Guillén P, Alcalde JG, García L, Bilbao R (2008) Toluene steam reforming using coprecipitated Ni/Al catalysts modified with lanthanum or cobalt. Chem Eng J 137: 587-597.
15. Garbarinoa G, Wang CY, Valsamakisb I, Chitsazana S, Rianic P, et al. (2015) A study of Ni/Al_2O_3 and Ni-La/Al_2O_3 catalysts for the steam reforming of ethanol and phenol. Appl Catal B 174-175: 21-34.
16. Polychronopoulou K, Fierro JLG, Efstathiou AM (2004) The phenol steam reforming reaction over MgO-based supported Rh catalysts. J Catal 228: 417-432.
17. Coronel L, Múnera JF, Tarditi AM (2014) Hydrogen production by ethanol steam reforming over Rh nanoparticles supported on lanthana/silica systems. Appl Catal B 160-161: 254-266.
18. Suzuki T, Iwanami H, Yoshinari T (2000) Steam reforming of kerosene on Ru/Al_2O_3 catalyst to yield hydrogen. Int J Hydrog Energy 25: 119-126.
19. Cassinelli WH, Damyanova S, Parizotto NV (2014) Study of the properties of supported Pd catalysts for steam and autothermal reforming of methane. Appl Catal A 475: 256-269.
20. Hou T, Zhang S, Xu T (2014) Hydrogen production from oxidative steam reforming of ethanol over Ir/CeO_2 catalysts in a micro-channel reactor. ChemEng J 255: 149-155.
21. Furusawaa T and Tsutsumi A (2005) Comparison of Co/MgO and Ni/MgO catalysts for the steam reforming of naphthalene as a model compound of tar derived from biomass gasification. Appl Catal A 278: 207-212.

22. Parka HJ, Parkb SH, Sohnc JM, Parkd J, Jeone J, et al. (2010) Steam reforming of biomass gasification tar using benzene as a model compound over various Ni supported metal oxide catalysts. Bioresour Technol 101: S101-S103.

23. Urasaki K, Tokunaga K, Sekine Y, Matsukata M, Kikuchi E (2008) Production of hydrogen by steam reforming of ethanol over cobalt and nickel catalysts supported on perovskite-type oxides. Catal Commun 9: 600-604.

24. Wanga L, Lia D, Koikea M, Watanabeb H, Xuc Y, Nakagawaa Y, Tomishige K (2013) Catalytic performance and characterization of Ni-Co catalysts for the steam reforming of biomass tar to synthesis gas. Fuel 112: 654-661.

25. Iwasaa N, Yamanea T, Takeib M, Ozakib J, Arai M (2010) Hydrogen production by steam reforming of acetic acid: Comparison of conventional supported metal catalysts and metal-incorporated mesoporous smectite-like catalysts. Int J Hydrogen Energy 35: 110-117.

26. Urasaki K, Tokunaga K, Sekine Y, Matsukata M, Kikuchi E (2015) Steam reforming of biomass tar model compound at relatively low steam-to-carbon condition over CaO-doped nickel-iron alloy supported over iron-alumina catalysts. Appl Catal A 490: 24-35.

27. Zhang RQ, Wang H, Hou X (2014) Catalytic reforming of toluene as tar model compound: effect of Ce and Ce-Mg promoter using Ni/olivine catalyst. Chemosphere 97: 40-46.

28. Mukaia D, Tochiya S, Murai Y, Imoria M, Sugiura Y, et al. (2013) Structure and activity of $Ni/La_{0.7}Sr_{0.3}AlO_{3-\delta}$ catalyst for hydrogen production by steam reforming of toluene. Appl Catal A 464-465: 78-86.

29. Swierczynski D, Libs S, Courson C, Kiennemann A (2007) Steam reforming of tar from a biomass gasification process over Ni/olivine catalyst using toluene as a model compound. Appl Catal B 74: 211-222.

30. Mukaia D, Muraia Y, Higoa T, Tochiyaa S, Hashimotoa T, et al. (2013) In situ IR study for elucidating reaction mechanism of toluene steam reforming over $Ni/La_{0.7}Sr_{0.3}AlO_{3-\delta}$ catalyst. Appl Catal A 466:190-197.

31. Sun NN, Wen X,Wang F, Wei W, Sun YH (2010) Effect of pore structure on Ni catalyst for CO_2 reforming of CH_4. Energy Environ Sci 3: 366-369.

32. Yu XP, Chu W, Wang N, Ma F (2011) Hydrogen Production by Ethanol Steam Reforming on NiCuMgAl Catalysts Derived from Hydrotalcite-Like Precursors. Catal Lett 141: 1228-1236.

33. Zhang CX, Yue HR, Huang ZQ, Li SR, Wu GW, et al. (2012) Hydrogen Production via Steam Reforming of Ethanol on Phyllosilicate-Derived Ni/SiO_2: Enhanced Metal-Support Interaction and Catalytic Stability. ACS Sustain ChemEng 1: 161-173.

34. Nichele V, Signoretto M, Menegazzo F, Rossetti I, Cruciani G (2014) Hydrogen production by ethanol steam reforming: Effect of the synthesis parameters on the activity of Ni/TiO_2 catalysts. Int J Hydrogen Energy 39: 4252-4258.

35. Deshmanea VG, Owena SL, Abrokwahc RY, Kuila D (2015) Mesoporous nanocrystalline TiO_2 supported metal (Cu, Co, Ni, Pd, Zn, and Sn) catalysts: Effect of metal-support interactions on steam reforming of methanol. J MolCatal a Chem 408: 202-213.

36. Li TT, Zhang JF, Xie M, Yin XM, An X (2015) Montmorillonite-supported Ni nanoparticles for efficient hydrogen production from ethanol steam reforming. Fuel 143: 55-62.

37. Burattin P, Che M, Louis C (1999) Metal Particle Size in Ni/SiO_2 Materials Prepared by Deposition-Precipitation: Influence of the Nature of the Ni(II) Phase and of Its Interaction with the Support. J Phys Chem B 103: 6171-6178.

38. Burattin P, Che M, Louis C (2000) Ni/SiO_2 Materials Prepared by Deposition-Precipitation: Influence of the Reduction Conditions and Mechanism of Formation of Metal Particles. J Phys Chem B 104: 10482-10489.

39. Burattin P, Che M, Louis C (1998) Molecular Approach to the Mechanism of Deposition-Precipitation of the Ni(II) Phase on Silica. J PhysChem B 102: 2722-2732.

40. Wu T, Zhang Q, Cai W, Zhang P, Song XF, Sun Z, Gao L (2015) Phyllosilicate evolved hierarchical Ni- and Cu-Ni/SiO_2 nanocomposites for methane dry reforming catalysis. Appl Catal A 503: 94-102.

41. Sivaiaha MV, Petitb S, Barraulta J, Batiot-Dupeyrata C, Valangea S (2010) CO_2 reforming of CH_4 over Ni-containing phyllosilicates as catalyst precursors. Catal Today 157: 397-403.

42. Kong X, Zhu YF, Zheng HY (2015) Ni Nanoparticles Inlaid Nickel Phyllosilicate as a Metal-Acid Bifunctional Catalyst for Low-Temperature Hydrogenolysis Reactions. ACS Catal 5: 5914-5920.

43. Quitetea CPB, Bittencourta RCP, Souzab MM (2014) Steam reforming of tar using toluene as a model compound with nickel catalysts supported on hexaaluminates. Appl Catal A 478: 234-240.

44. Baidya T, Cattolica RJ (2015) Fe and CaO promoted Ni catalyst on gasifier bed material for tar removal from producer gas. Appl Catal A 503: 43-50.

45. Heo DH, Lee R, Hwang JH, Sohn JM (2015) The effect of addition of Ca, K and Mn over Ni-based catalyst on steam reforming of toluene as model tar compound. Catal Today 265: 95-102.